XLIII CILAMCE
21–25, November, 2022
FOZ DO IGUAÇU – PR – BRAZIL

On a kinematically exact rod model for thin-walled open section members: incorporating polyconvex constitutive equation

Marcos P. Kassab[1], Eduardo M. B. Campello[1], Paulo M. Pimenta[1]

[1]*Dept. of Structural and Geotechical Engineering, Polytechnic School, University of São Paulo*
P.O. Box 61548, 05424-970, São Paulo, Brazil
marcos.kassab@usp.br, campello@usp.br, ppimenta@usp.br

Abstract. In the current work, advances on kinematically exact rod models for thin-walled open section members, taking into account both primary and secondary cross-sectional warpings, are proposed. Advanced elastic constitutive equations are incorporated in order to enable full bending, compression and torsional strain couplings in the finite strain regime. The paper extends a previous contribution by the authors (Kassab and Campello [1] "On a kinematically exact rod model for thin-walled open section members", CILAMCE-PANACM-2021) by incorporating a more advanced constitutive equation, now based on the polyconvex neo-Hookean Simo-Ciarlet's material. The older version contemplated only linear elastic and Saint-Venant´s constitutive equations, which are known for being unsuited for truly finite strains. Differently from what was performed in a past attempt, all the terms of the constitutive equation were retained. The model was implemented in PEFSYS, which is an in-house FEM program. Validation is performed using existing results from the literature as well as solutions obtained with the Ansys's shell 281 element.

Keywords: Kinematically exact rod models, thin-walled rods, polyconvex constitutive equation

1 Introduction

Kinematically exact models attempt to correctly describe structures undergoing finite displacements. They are suitable for situations in which large deformation occurs, even allowing the evaluation of critical loads and post-critical behaviour.

The first consistent 3D exact rod model was proposed by Simo [2], [3], that imposed rigid cross-section assumptions. Later, Simo and Vu-Quoc [4] also advanced towards a model with warping considerations, especially useful for torsion-dominated problems. A wide array of nonlinear rod models has been developed in the literature since then, many of them derived directly from Simo's works. In order to mention a few interesting formulations, particularly related to the purpose of this paper, the reader might consult the works of Crisfield [5], Pimenta and Yojo [6], Campello [7], Pimenta and Campello [8, 9], Dasambiagio et al. [10], Campello and Lago [11], Le Corvec [12], among many others.

For thin-walled open-section members, the associated rod formulations must take cross-sectional warping into account, since it becomes a relevant load-carrying mechanism due to the very small torsion stiffness of such members. For this work, advances on kinematically exact rod models for thin-walled open section members are proposed, taking into account both primary and secondary cross-sectional warpings. In a previous work Kassab and Campello [1]), the author discussed the importance of adequately treating the description of primary and secondary warping for the correct stress integration, mainly when advanced constitutive equations are employed. In that work, the Saint-Venant's material was used – it is considered a finite deformation-small strain material, as it can be proven that, for specific extreme strains, it might not admit a solution (see Raoult [13]). As an extension of that work, an equivalent implementation of the rod model is done here, using the exact expression of the polyconvex Simo-Ciarlet's material, which is a large deformation-large strain material.

The incorporation of such advanced elastic constitutive equations enabled full bending, compression and torsional strain couplings in the finite strain regime. For thin-walled open-section members with linear elastic material, the warping effects are fully characterized by the well-known torsion inertia (from the Saint-Venant's uniform torsion theory) and the warping constant (from the Vlasov's theory Vlasov [14]). The former has a well-known analytic expression, whilst the latter is obtained only considering the so-called primary warping, which is the warping in the direction of the cross-section´s walls lengths. The walls´ thickness warping, or secondary

warping, is typically neglected. However, for more advanced constitutive equations, such as the ones of interest here, explicit knowledge of the warping and its directional derivatives at every point of the cross section are of utmost importance for the integration of the stress resultants – both primary and secondary cross-sectional components must be considered.

The model is implemented into PEFSYS, a nonlinear finite element program for static and dynamic analysis under development at the Department of Structural and Geotechnical Engineering of the University of São Paulo, and is validated against reference solutions obtained from the literature and also with ANSYS's shell 281 elements. This work is an intermediate step of a larger work, which aims to incorporate the truly large-strain, neo-Hookean Simo-Ciarlet's material law at the constitutive equation.

2 The rod model

The rod model of this paper uses total Lagrangean description. Its kinematics is based on the multi-parameter beam model from Pimenta and Campello Pimenta and Campello [9] (see also Dasambiagio et al. [10]), imposing the assumption that the displacement field of a cross-section can be described by a rigid body displacement (defined by the beam axis´ displacements u and Euler rotation vector θ, on the global Cartesian system, comprising 6 DOFs), plus an out-of-plane displacement (warping). The latter is given by the product of a warping intensity parameter (p, the 7th DOF) and a shape function (ψ).

Two constitutive equations are derived: one from the Saint-Venant's material (as in Campello and Lago [11]) and the other from the Simo-Ciarlet's material (as in Pimenta and Campello [9], Dasambiagio et al. [10], but particularized for the current 7-DOF model). Here, the exact expressions are used (i.e. no strain contribution is neglected), opposed to the often used linear constitutive equation, as in Simo [2]-Simo and Vu-Quoc [4] and Pimenta and Yojo [6] or to Pimenta and Campello [8], where only some terms up to the second order are retained. To compute the stress resultants and material tangent matrix, the cross-section´s walls were discretized on rectangular cells, and then the desired function was integrated with the standard composed Simpson's method. The model was implemented with standard Lagrangean isoparametric beam finite element, numerically integrated along the element's axis with reduced integration to avoid shear locking. Incremental load steps are used for the solution – each one of them is solved using Newton's method.

2.1 Kinematical description

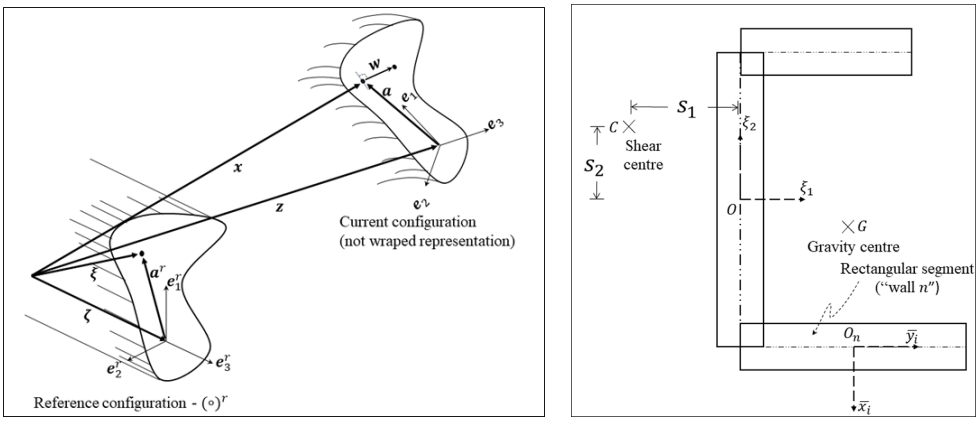

(a) (b)

Figure 1. (a) Rod kinematics and (b) representation of a thin-walled cross-section

Assuming a straight rod initial configuration, with a local orthonormal system $\{\boldsymbol{e}_1^r, \boldsymbol{e}_2^r, \boldsymbol{e}_3^r\}$, with $\boldsymbol{e}_3^r$ coinciding with the reference rod´s axis (see Fig. 1(a)), the position of every material point in the reference configuration ($\boldsymbol{\xi}$) and in the current configuration ($\boldsymbol{x}$) can be described by

$$\boldsymbol{\xi} = \zeta \boldsymbol{e}_3^r + \boldsymbol{a}^r,\ \zeta \in \Omega = [0, L], \tag{1}$$

$$\boldsymbol{x} = \boldsymbol{z} + \boldsymbol{a} + \boldsymbol{w}, \tag{2}$$

where $\boldsymbol{u} = \boldsymbol{z} - \boldsymbol{\zeta}$ is the displacement of the reference axis, $\boldsymbol{a} = \boldsymbol{Q}\boldsymbol{a}^r$ is the cross-sectional displacements due to rotation ($\boldsymbol{Q}$ is the rotation tensor) and $\boldsymbol{w} = p\psi\boldsymbol{e}_3$ is the warping displacement, for a warping function (ψ) and a warping intensity (p). For each cross-sectional wall n, an orthonormal local system ($\bar{x}_n, \bar{y}_n$) is assigned (see Fig. 1(b)), as this will be useful for the definition of the warping function later on. The rotation tensor is parametrized using Euler-Rodrigues equation, exactly as done in Simo [2], Pimenta and Yojo [6], Campello [7], for example. It is useful to group the model´s DOFs into a generalized displacement vector, $\boldsymbol{d} = [\boldsymbol{u}, \boldsymbol{\theta}, p]^T$. The deformation gradient $\boldsymbol{F}$ is obtained from eq. (2), and reads

$$\begin{gathered}\boldsymbol{F} = \frac{\partial \boldsymbol{x}}{\partial \boldsymbol{\xi}} = \boldsymbol{Q}(\boldsymbol{I} + \psi_{,\alpha} p \boldsymbol{e}_3^r \otimes \boldsymbol{e}_\alpha^r + \boldsymbol{\gamma}^r \otimes \boldsymbol{e}_3^r) = \boldsymbol{Q}\boldsymbol{F}^r \text{ , with} \\ \boldsymbol{\gamma}^r = \boldsymbol{\eta}^r + \boldsymbol{\kappa}^r \times (\boldsymbol{a}^r + \psi p \boldsymbol{e}_3^r) + \psi p' \boldsymbol{e}_3^r \text{ and } \boldsymbol{\eta}^r = \boldsymbol{Q}^T \boldsymbol{z}' - \boldsymbol{e}_3^r \text{ and } \boldsymbol{\kappa}^r = \boldsymbol{\Gamma}\boldsymbol{\theta}'.\end{gathered} \tag{3}$$

Tensor $\boldsymbol{\Gamma}$, required in eq. (3), is a sub-product of the derivative of the rotation tensor, and its definition can be found in Simo [2] (with a different notation), or in Pimenta and Yojo [6]. The above strain quantities can be assigned to a generalized strain vector, $\boldsymbol{\varepsilon}^r = [\boldsymbol{\eta}^r \ \boldsymbol{\kappa}^r \ p \ \ p']^T$.

The adopted warping function is, for each wall n

$$\begin{gathered}\psi\left(\xi_1, \xi_2\right) = \psi_L(\xi_1, \xi_2) + \psi_R\left(\bar{x}_n, \bar{y}_n\right) \\ \psi_L\left(\xi_1, \xi_2\right) = -(s_2 - O_n^{\xi_2})\left(\xi_1 \ - O_n^{\xi_1}\right) + (s_1 - O_n^{\xi_1})\left(\xi_2 - O_n^{\xi_2}\right) + c_n,\end{gathered} \tag{4}$$

where $\psi_R\left(\bar{x}_n, \bar{y}_n\right)$ is a polynomial approximation of the Saint-Venant's warping function for a rectangle, w.r.t its centroid (from Silva [15]), (s_1, s_2) are the coordinates of the section´s shear centre and $(O_n^{x_1}, O_n^{x_2})$ the coordinates of the wall´s centroid. This function was proposed by the author, and recovers satisfactorily the Saint-Venant's warping function for open-section thin-walled members (see Kassab and Campello [1] for details). It should be highlighted that eq. (4) is an advancement from what was previously proposed in Campello and Lago [11].

2.2 Equilibrium: weak form

The virtual work theorem is invoked, imposing the rod´s equilibrium:

$$\delta W = \delta W_{int} - \delta W_{ext} = 0 \text{ in } \Omega, \ \forall \delta \boldsymbol{d} | \boldsymbol{d}(0) = \boldsymbol{d}(L) = \boldsymbol{o}, \tag{5}$$

with

$$\begin{gathered}\delta W_{int} = \int_\Omega \int_{A^r} \boldsymbol{P} : \delta \boldsymbol{F} dA^r d\zeta = \int_\Omega (\boldsymbol{\sigma}^r \cdot \delta \boldsymbol{\varepsilon}^r) d\zeta, \text{and} \\ \delta W_{ext} = \int_\Omega (\bar{\boldsymbol{q}} \cdot \delta \boldsymbol{d}) d\zeta,\end{gathered} \tag{6}$$

wherein $\boldsymbol{\sigma}^r = [\boldsymbol{n}^r, \boldsymbol{m}^r, Q, B]^T$ is the generalized back-rotated stress resultants vector (obtained through cross-sectional integration of the column-vectors of the back-rotated stresses $\boldsymbol{P}^r = \boldsymbol{Q}^T\boldsymbol{P}$ (see Campello and Lago [11])), $\delta\boldsymbol{\varepsilon}^r = \boldsymbol{\Psi}\boldsymbol{\Delta}\delta\boldsymbol{d}$ has an analogous definition as $\boldsymbol{\varepsilon}^r$ ($\boldsymbol{\Psi}$ and $\boldsymbol{\Delta}$ are auxiliary operators that contain derivatives of rotation and strain tensors and derivation operators, see Simo [2]) and $\bar{\boldsymbol{q}} = \left[\bar{\boldsymbol{n}}, \bar{\boldsymbol{\mu}}, \ \bar{B}\right]^T$ is the vector of external loads. Note that $\bar{\boldsymbol{\mu}} = \boldsymbol{\Gamma}^T\bar{\boldsymbol{m}}$ is the pseudo-moment, which is conjugated to the virtual rotations, instead of the moment itself, see Simo [2], Simo and Vu-Quoc [3], Pimenta and Yojo [6] for more details. The interpretation of those quantities is the usual: vector $\boldsymbol{n}$ contains the shear and axial forces, whereas $\boldsymbol{m}$ contains the bending and torsional moments. The warping-related resultants are the bi-shear (Q) and bi-moment (B). These stress resultants are obtained through cross-sectional integration of the column-vectors ($\boldsymbol{\tau}_i^r$) of the back-rotated stresses $\boldsymbol{P}^r = \boldsymbol{Q}^T\boldsymbol{P} = \boldsymbol{\tau}_i^r \otimes \boldsymbol{e}_i^r$, as in Campello and Lago [11].

Consistent linearization of eq. (5) with respect to $\boldsymbol{d}$ results in the tangent operator of the equilibrium, and will be directly used on the finite element method's formulation, as already reported in Simo [2], Pimenta and Yojo [6], Pimenta and Campello [8] and other references that use a similar description for their models.

2.3 Constitutive equation

In this work, the model was implemented with the exact (i.e., all strain terms retained) expression of both the Saint-Venant's and Simo-Ciarlet's material laws. The former can be seen in Campello and Lago [11] (although presented in a slightly different fashion), whilst the latter is

$$\boldsymbol{\tau}_i^r = \left[\frac{\lambda}{2}\left(J - \frac{1}{J}\right) - \mu\frac{1}{J}\right]\boldsymbol{g}_i^r + \mu\boldsymbol{f}_i^r, \tag{7}$$

where $\boldsymbol{f}_i^r$ represent the column-vectors of $\boldsymbol{F}^r$, $J = det\boldsymbol{F}$, $\boldsymbol{g}_i^r = \frac{1}{2}\epsilon_{ijk}\boldsymbol{f}_j^r \times \boldsymbol{f}_k^r$ (ϵ_{ijk} is the permutation symbol) and (λ, μ) are the Lamé constants for the pair $\boldsymbol{S}$, $\boldsymbol{E}$. Equation [7] is a particularization of the expression for general cross-sectional distortion from Pimenta and Campello [9], Dasambiagio et al. [10]. Using this exact expression of eq. (7), one can compute the stress resultants $\boldsymbol{\sigma}^r$ and the material tangent matrix $\boldsymbol{D} = \frac{\partial\boldsymbol{\sigma}^r}{\partial\boldsymbol{\varepsilon}^r}$ with no simplifications (please consult Pimenta and Campello [9], Dasambiagio et al. [10], Campello and Lago [11] for details).

Due to the kinematical assumptions, Poisson's effects must be ignored, to avoid volumetric locking. Therefore, the expressions $\mu = G$ and $\lambda + 2\mu \simeq E$ are used to derive the Lamé's constants from the Young's and shear moduli. The matrix of elastic tangent moduli $\boldsymbol{D}$ can also be obtained for this elastic constitutive equation. A detailed description of its components can be found in Campello and Lago [11]. It is also important to reiterate that, in the current formulation, $\boldsymbol{\tau}_i^r$, $\boldsymbol{\sigma}^r$ and $\boldsymbol{D}$ are written in their exact forms, with no simplifications. Strain coupling involving higher-order strain terms can be seen when the exact forms are used (some authors refer to some of those terms as "Wagner terms"). In the context of thin-walled open section members, it is especially important to highlight the coupling between torsional and warping strains (κ_3^r, p and p') with axial and bending strains (η_3^r and κ_α^r), despite the fact that all the terms from $\boldsymbol{\varepsilon}^r$ are intertwined.

The importance of implementing the Simo-Ciarlet's material resides on the fact that, unlike the Saint-Venant's material, it is polyconvex. Polyconvexity is a sufficient condition for the existence of solution for the minimization of the potential energy (strictly speaking, such condition is only valid for conservative problems), avoiding issues with material stability (for more details about this subject, consult Ciarlet [16] or Ball [17]). This is specially useful for compression-dominated problems, since it is known that the Saint-Venant's material might present a pathological behaviour in extreme compression situations. By having a rod model that complies with the polyconvexity condition, one does not need to face any kind of *material* instabilities.

3 Numerical examples

In this section we provide illustrative examples to show the current model's applicability on simple general situations. We consider elastic rods with $E = 200\,GPa$ and $G = 80\,GPa$ (except on the C-section of example 3.1, where $E = 210\,GPa$ was used to be consistent with Gruttmann et al. [18]). The results from the two studied materials (Saint-Venant's and Simo-Ciarlet's) are compared with reference solutions using kinematically exact rod models linear elastic material, either from the literature or implemented in PEFSYS (see Pimenta and Campello [8], Campello [7] for details), and also with Ansys's shell models for large deformations and linear elasticity. For examples with pre-critical loading, analytical solutions from Vlasov [14] are also reported for comparison. In order to transpose bifurcation points in post-critical analyses, a load perturbation of 1% of the main load was applied. In all cases, the rods were homogeneously discretized in 10 linear (i.e., 2-node) elements (the only exception, again, is the C-section from example 3.1, with 30 elements), and the cross-sectional walls in 10x30 integration cells.

3.1 Bending and torsion of beams in small to moderate (pre-critical) loading

In this section, two examples are explored: A) the first example is a simply supported I-section (see Fig. 2(a)) beam, of lenght $L = 500\ cm$. The reference axis is placed on the centroid of the cross-section with, the following boundary conditions: i) torsion rotation restricted at the edges; ii) free warping at the edges; iii) uniformly distributed vertical load $p = -0.215\,kN/cm$ and distributed torsional moment $m = 0.688\,kNcm/cm$. B) the second example is a C-section cantilever (see Fig. 3(a)), of lenght $L = 900\,cm$. The reference axis is placed on the web/top flange intersection, with the following boundary conditions: i) a clamped end and b) a transversal vertical load at the free tip (out of the shear centre - torsion is naturally expected to occur). This load is incremented from $P = 0$ to $20\,kN$. Those examples do not contemplate any instabilities, but large deformation does occur in the second case.

As it can be seen in Figs. 2(b) and 2(c), results for the I-beam are almost coincident to Vlasov's analytical solution and to ANSYS´s shell solution. It should be noted that first order terms of both Saint-Venant's and Simo-Ciarlet's materials are equivalent to linear elastic one, justifying this adherence in this small strains and displacements case.

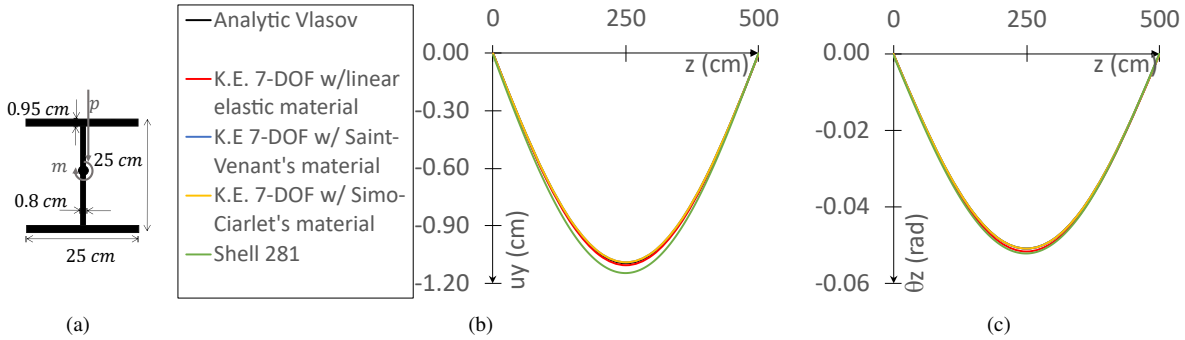

Figure 2. a) I-section definition, b) vertical displacement, c) torsional rotation for example 3.1 (A)

For the cantilever, with markedly larger final displacements, there is a load level when both geometrical and material nonlinearities turn relevant (see Figs. 3(b) and 3(c)). Up to $P \approx 8\,kN$, the vertical displacement (u_y) and torsional rotation (θ_z) are almost coincident for nearly all models, including the analytical Vlasov's solution. After this load level, there is a change in the load-carrying mechanism and the deformation is intensified (yet, it should be remarked that this is NOT a buckling case). From this level and beyond on, the rod models simulated with PEFSYS proved stiffer than those from Gruttmann et al. [18], despite the kinematical formulation from the former being rather equivalent to the linear elastic model from Campello [7]. Further investigation have shown that relevant in-plane distortional displacements are present near the clamped end, rendering the in-plane rigid assumption rather flawed. A discussion about the inclusion of distortional modes on rod models can be seem in Li and Ma [19]. In this reference, there are some similar C-channels, in which this phenomenon is also detected. The models with Saint-Venant's and Simo-Ciarlet's material presented the same result, both showing an influence of strain coupling effects, which the linear elastic material model was unable to identify.

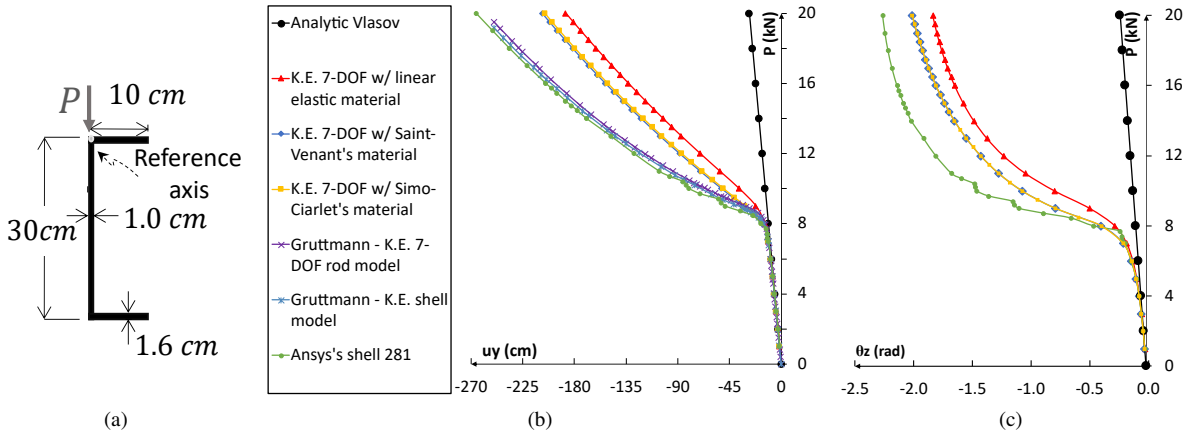

Figure 3. a) C-section definition, b) vertical displacement, c) torsional rotation for example 3.1 (B)

3.2 Buckling and post-critical analysis of an I-section column and beam) loading

This example deals with the buckling of a clamped I-section rod (see (Fig. 4(a)), with a load at the centroid of the free end. Two cases are studied (i) compressed column and (ii) transversely-loaded beam. As it can be seen in (Fig. 4(b)) and (Fig. 4(c)), the current model is able to correctly identify the critical load. For the compression case, all models presented nearly the same displacements on the post-critical regime. For the transverse load case, in the developed large-displacements regime, the influence of high-order strain coupling (notably between torsional and bending strains) is identified in models with both Saint-Venant's and Simo-Ciarlet's material, making

the results differ from those from the linear elastic rod and shell models. Again, it must be highlighted that the two hyperelastic constitutive equations presented practically the same results.

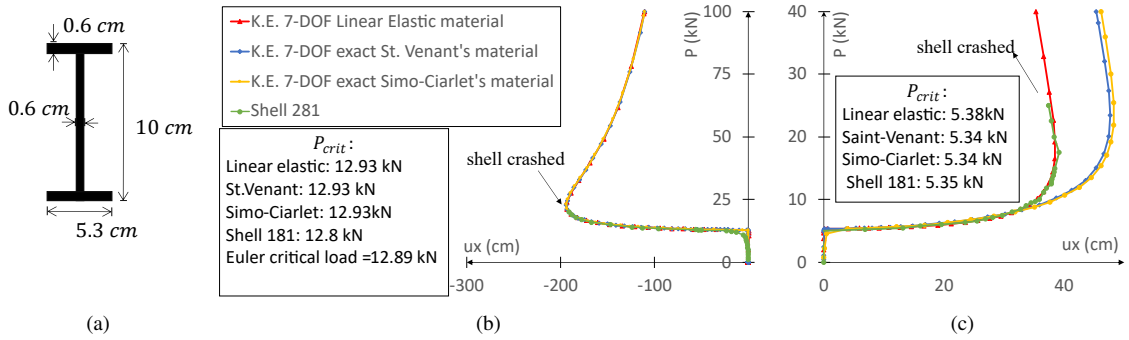

(a) (b) (c)

Figure 4. Problem description for example 3.2, lateral displacements for the (a) column and (b) beam

3.3 Torsional buckling of cruciform and T-section columns

This example is the torsional buckling of compressed clamped short columns of length l, with cruciform and T-shaped cross-sections as shown in Fig. 5(a). The compressive load is applied at the centroid of the free-end . As it can be seen in Fig. 5(b) and Fig. 5(c), the rod model with linear elastic material was always unable to identify the torsion buckling, whereas the models with any of the two hyperelastic materials (with full strain coupling) correctly identified the critical load. It must be said, however, that compared to the shell model, the post-critical torsional response herein obtained is significantly different. One possible explanation is that the shell model, as in section 3.1(B), is able to capture in-plane cross-sectional deformations (volumetric and distortional changes). Those are surely relevant in the post-critical regime for such short columns. As in all the previous cases, the two studied constitutive equations presented practically the same results.

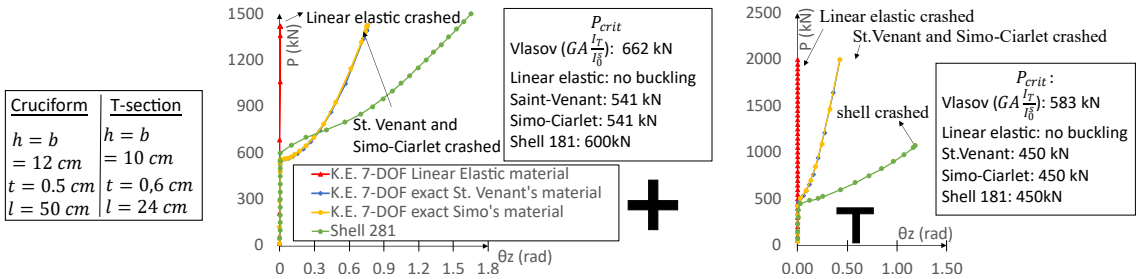

(a) (b) (c)

Figure 5. Problem description for example 3.3. Torsion rotation for (a) cruciform section and (b) T-section

4 Conclusions

Extension of a previous contribution from the author [1] was achieved: the Simo-Ciarlet's material polyconvex material was implemented on the context of kinematically exact 7-DOF models. The model was validated in pre-critical loading situations and buckling load determination, as well as in the post-critical regime. The coupling effects between torsion strains and other degrees of freedom proved crucial at the constitutive equation for proper torsional bucking representation, for both Saint-Venant's and Simo-Ciarlet's material. Despite being more suited to fully finite-strain situations, the Simo-Ciarlet's material rendered practically the same result as the Saint-Venant's material. It has become clear that kinematic restrictions are the bottleneck of the present formulation, as material stability is guaranteed due to the polyconvex constitutive equation.

Acknowledgements. This work was supported by FAPESP (São Paulo Research Foundation) – grant #2021/02042-9 – and CNPq (Conselho Nacional de Desenvolvimento Científico e Tecnológico) – grants #307368/2018-1 and

#313046/2021-2. The opinions, hypotheses, conclusions and recommendations expressed herein are the sole responsibility of the authors and do not necessarily reflect FAPESP's and CNPq´s visions.

Authorship statement. The authors hereby confirm that they are the sole liable persons responsible for the authorship of this work, and that all material that has been herein included as part of the present paper is either the property (and authorship) of the authors, or has the permission of the owners to be included here.

References

[1] M. P. Kassab and E. M. B. Campello. On a kinematically exact rod model for thin-walled open section members. pp. 7, Proceedings of the joint XLII Ibero-Latin-American Congress on Computational Methods in Engineering and III Pan-American Congress on Computational Mechanics, ABMEC-IACM, 2021.

[2] J. Simo. A finite strain beam formulation. The three-dimensional dynamic problem. Part I. *Computer Methods in Applied Mechanics and Engineering*, vol. 49, n. 1, pp. 55–70. Number: 1, 1985.

[3] J. Simo and L. Vu-Quoc. A three-dimensional finite-strain rod model. part II: Computational aspects. *Computer Methods in Applied Mechanics and Engineering*, vol. 58, n. 1, pp. 79–116. Number: 1, 1986.

[4] J. Simo and L. Vu-Quoc. A Geometrically-exact rod model incorporating shear and torsion-warping deformation. *International Journal of Solids and Structures*, vol. 27, n. 3, pp. 371–393. Number: 3, 1991.

[5] M. Crisfield. A consistent co-rotational formulation for non-linear, three-dimensional, beam-elements. *Computer Methods in Applied Mechanics and Engineering*, vol. 81, n. 2, pp. 131–150. Number: 2, 1990.

[6] P. M. Pimenta and T. Yojo. Geometrically Exact Analysis of Spatial Frames. *Applied Mechanics Reviews*, vol. 46, n. 11S, pp. S118–S128. Number: 11S, 1993.

[7] E. M. B. Campello. Análise não-linear de perfis metálicos conformados a frio. *São Paulo*, pp. 106, 2000.

[8] P. M. Pimenta and E. M. B. Campello. Geometrically nonlinear analysis of thin-walled space frames. pp. 20, Proceedings of the II ECCM (European Conference on Computational Mechanics), 2001.

[9] P. M. Pimenta and E. M. B. Campello. A fully nonlinear multi-parameter rod model incorporating general cross-sectional in-plane changes and out-of-plane warping. *Latin American Journal of Solids and Structures*, pp. 22, 2003.

[10] E. R. Dasambiagio, P. M. Pimenta, and E. M. B. Campello. A finite strain rod model that incorporates general cross section deformation and its implementation by the Finite Element Method. In H. S. da Costa Mattos and M. Alves, eds, *Mechanics of Solids in Brazil 2009*, volume 1, pp. 145–168. Brazilian Society of Mechanical Sciences and Engineering, Rio de Janeiro, 1 edition, 2009.

[11] E. M. Campello and L. B. Lago. Effect of higher order constitutive terms on the elastic buckling of thin-walled rods. *Thin-Walled Structures*, vol. 77, pp. 8–16, 2014.

[12] V. Le Corvec. *Nonlinear 3d frame element with multi-axial coupling under consideration of local effects*. Dissertation, University of California, Berkeley, 2012.

[13] A. Raoult. Non-polyconvexity of the stored energy function of a saint venant-kirchhoff material. *Applications of Mathematics*, pp. 417–419, 1986.

[14] V. Z. Vlasov. *Thin-walled Elastic Beams*. Israel Program for Scientific Translation, Jerusalem, 2nd edition, 1961.

[15] H. F. Silva. *Formulação do problema da torção uniforme em barras de seção transversal maciça.* Mestrado em Engenharia de Estruturas, Universidade de São Paulo, São Paulo, 2005.

[16] P. G. Ciarlet. *Mathematical elasticity*. Number v. 20, 27, 29 in Studies in mathematics and its applications. North-Holland ; Sole distributors for the U.S.A. and Canada, Elsevier Science Pub. Co, Amsterdam ; New York : New York, N.Y., U.S.A, 1988.

[17] J. M. Ball. Convexity conditions and existence theorems in nonlinear elasticity. *Archive for Rational Mechanics and Analysis*, vol. 63, n. 4, pp. 337–403. Number: 4, 1976.

[18] F. Gruttmann, R. Sauer, and W. Wagner. Theory and numerics of three–dimensional beams with elastoplastic material behaviour. *International Journal for Numerical Methods in Engineering*, pp. 33, 2000.

[19] W. Li and H. Ma. A nonlinear cross-section deformable thin-walled beam finite element model with high-order interpolation of warping displacement. *Thin-Walled Structures*, vol. 152, pp. 106748, 2020.